

# Squeezing Bi: PNP and $P_2N_3$ pincer complexes of Bismuth(III)

Marcus B. Kindervater,<sup>a†</sup> Toren Hynes,<sup>a†</sup> Katherine M. Marczenko,<sup>a</sup> Saurabh S. Chitnis<sup>a\*</sup>

<sup>a</sup> Department of Chemistry, Dalhousie University, 6274 Coburg Road, Halifax, Nova Scotia, B3H 4R2, Canada. E-mail: [saurabh.chitnis@dal.ca](mailto:saurabh.chitnis@dal.ca)

<sup>†</sup> Equal Contributions

## Abstract

We report the first application of a rigid  $P_2N_3$  pincer ligand in p-block chemistry by preparing its bismuth complex. We also report the first example of bismuth complexes featuring a flexible *PNP* pincer ligand, which shows phase-dependent structural dynamics. Highly electrophilic, albeit thermally unstable, Bi(III) complexes of the *PNP* ligand were also prepared.

The ability of tethered multi-dentate ligands to dictate structural outcomes is a powerful design strategy in coordination chemistry across the periodic table. Due to the relationship between frontier molecular orbitals and molecular symmetry, geometric distortion at main group element centres using multi-dentate ligands can elicit new reactivity, with applications in small molecule activation and catalysis.<sup>1-10</sup> A vast array of monoanionic tridentate ligands ( $L_2X$ , where L denotes a neutral donor and X an anionic substituent) – known as pincer ligands – have now been developed in the context of transition metal catalysis and, in principle, are all amenable to translation into p-block chemistry, enabling exquisite geometric tuning.

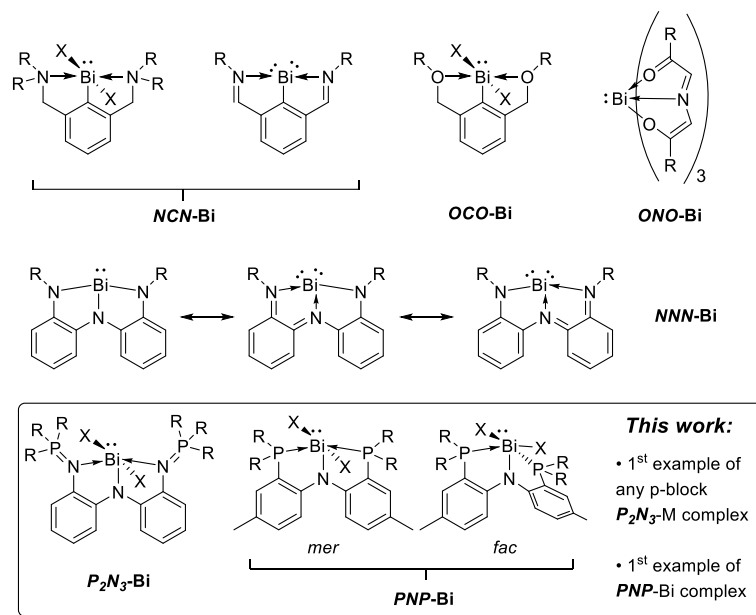


**Figure 1.** Monoanionic tridentate ( $L_2X$ , pincer) complexes of bismuth.

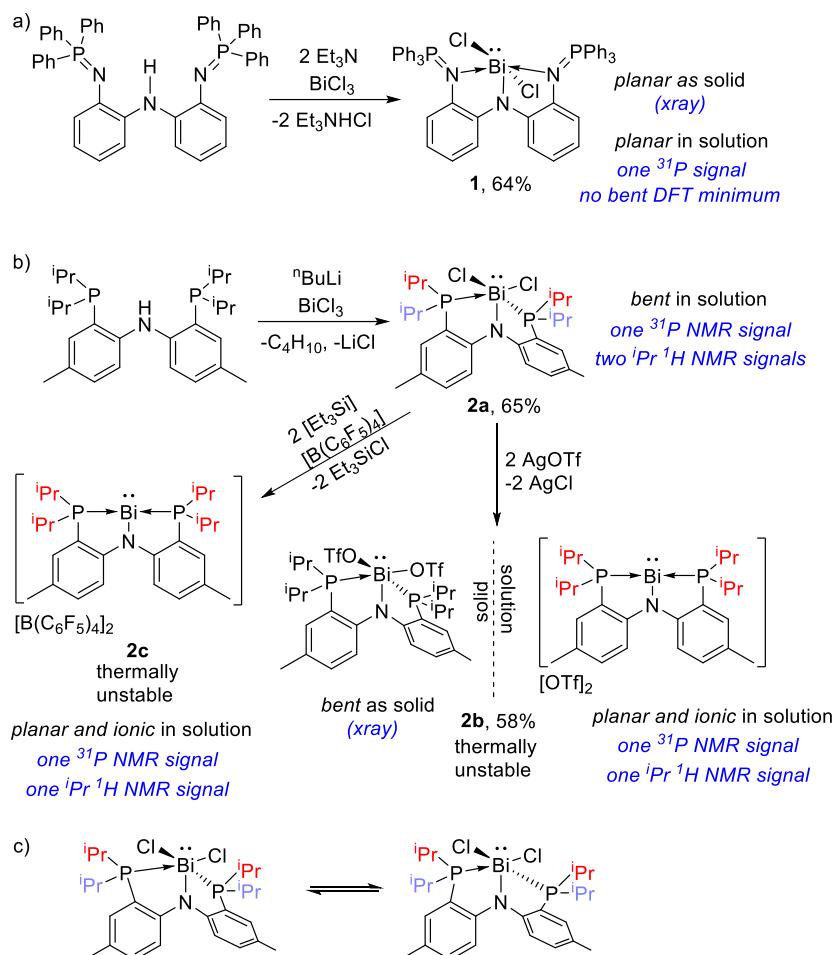
We are interested in rational frontier orbital engineering at heavy main group centres through such geometric perturbations.<sup>11-14</sup> Considering the  $L_2X$  pincer ligand coordination chemistry of bismuth (Figure 1), we noted that this area is dominated by the use of the **NCN** motif based on 2,5-substituted aryl groups.<sup>15-26</sup> Planar **NCN-Bi** complexes have been shown to activate challenging small molecules<sup>19, 20, 27</sup> and, more recently, found applications in hydrogen transfer catalysis.<sup>28, 29</sup> Rare example of **ONO-Bi** and **OCO-Bi** pincer complexes have also been isolated.<sup>30, 31</sup> The use of monoanionic **NNN** pincer ligands at Bi has been minimally explored by comparison.<sup>32</sup> In this context, we recently reported complex **NNN-Bi**, where a trianionic substituent undergoes intramolecular oxidation to become monoanionic, concomitant with reduction of the chelated Bi(III) centre to a formal Bi(I) oxidation state, as deduced from spectroscopic analysis and reactivity studies.<sup>11, 13</sup> In seeking to further evolve the pincer ligand

chemistry of bismuth, we have now explored the use of two new frameworks that are little-studied in p-block chemistry and unknown in bismuth chemistry.

The first is the amido-diphosphorane framework ( $P_2N_3$ ),<sup>33</sup> that is a monoanionic analogue of the formally trianionic ligand in **NMM-Bi**. While this rigidly planar  $P_2N_3$  ligand has been installed at a variety of d-block and f-block metals,<sup>34-41</sup> no p-block complex has to-date been reported. We hypothesized that the planarity evidenced in its d/f-block complexes would translate smoothly to bismuth. The second is a **PNP** ligand<sup>42</sup> whose application in p-block chemistry is also limited.<sup>43-50</sup> This ligand is more flexible than its  $P_2N_3$  counterpart, as demonstrated by the different coordination modes observed in **PNP-M** complexes: planar for M = Al, Ga, In or Sn;<sup>44, 45, 47</sup> bent when M = Li or P;<sup>43, 50</sup> and bidentate when M = B.<sup>49</sup> Given the metal size dependence of these coordination outcomes, we hypothesized that **PNP-Bi** complexes would also be planar due to the large size of the metal. Besides their geometric features, this pair of ligands is further appealing due to the presence of an NMR-responsive <sup>31</sup>P nuclei, which should facilitate analysis.

Here we debut these ligands in the coordination chemistry of bismuth by making the first complexes featuring the  **$P_2N_3$ -Bi** and **PNP-Bi** environments and show the varying degrees of planarity engendered through usage of the respective ligand. In the **PNP** case we further demonstrate the ability to support highly electrophilic Bi(III) centres that show the potential for Lewis acid catalysis.

Reaction of  **$P_2N_3$ -H** or **PNP-H** with BiCl<sub>3</sub> as per Scheme 1a gave compounds **1** and **2a**, respectively, as dark red solids in 64% and 65% yield. Compound **1** exhibits good solubility in a range of organic solvents and has therefore been fully characterized in solution and the solid state. The <sup>31</sup>P NMR spectrum of **1** shows a sharp singlet at 23.3 ppm and the <sup>1</sup>H and <sup>13</sup>C NMR spectra suggest a C<sub>2</sub> ligand symmetry with equivalent phosphinimine environments. Single crystals of **1** were obtained from a saturated DCM solution at -30 °C and confirmed the meridional arrangement inferred from solution NMR data (Figure 2a, Table 1). The coordination environment around Bi is best-described as a square-based pyramid with a stereochemically-active lone pair *trans* to the Bi-N1 bond. The N2-Bi-N3 angle of 146.6(2)° is significantly more compressed than the Cl-Bi-Cl angle of 175.75(5)°, due to the tethered nature of the  $P_2N_3$  ligand framework. The pnictogen core of **1** is almost perfectly planar confirming the very rigid nature of this ligand. The considerable steric bulk of the phosphinimine sidearms is evident in a space-filling view (Figure 2b), which presumably also explains why a bent orientation placing the sidearms *cis* to one another is not feasible. Consistently, several attempts to optimize a bent isomer through density functional theory (DFT) computations also failed to yield a stable minimum, converging instead to the planar structure.



**Scheme 1** Syntheses of **1**, **2a-c**, and considered mode of structural dynamism in **2a**.

In contrast to **1**, the *PNP*-ligated compound **2a** proved to be very poorly soluble, limiting solution phase characterization to  $^1\text{H}$  NMR and  $^{31}\text{P}$  NMR spectroscopy. At ambient temperature, **2a** shows a single broad peak at 41.3 ppm in the  $^{31}\text{P}$  NMR spectrum and the  $^1\text{H}$  NMR spectrum shows two very broad but distinct resonances for inequivalent isopropyl methine groups (Figure 3), indicating loss of planarity. We hypothesize that the signal broadening is the result of a dynamic process that involves an asymmetry in the strength of the two Bi-P interactions (Scheme 1c), as reported already in some *PNP-B* and *PNP-P* complexes.<sup>49, 50</sup> A variable temperature NMR study of **2a** was conducted, revealing partial resolution of the broad room temperature  $^{31}\text{P}$  NMR resonance into multiple overlapping signals at 193 K (Figure S13, ESI). The low temperature  $^1\text{H}$  NMR spectrum also shows two distinct environments for the isopropyl methine protons (Figure S14, ESI). An activation barrier of 58.8 kJ mol<sup>-1</sup> (14.0 kcal mol<sup>-1</sup>) was estimated from the coalescence temperature, but due to the small peak separation even at the lowest temperature

(solubility limited), multiplet analysis cannot be performed. Therefore, detailed discussion of the nature of the solution-phase dynamism is not possible at present, particularly because dimerization equilibria may also be operative in the low temperature regime.<sup>51, 52</sup> Nevertheless, taking the detection of two <sup>1</sup>Pr environment into account, we propose that the bent isomer is dominant in solution. Several attempts to characterize **2a** in the solid state were foiled by the low-quality of the crystals obtained.

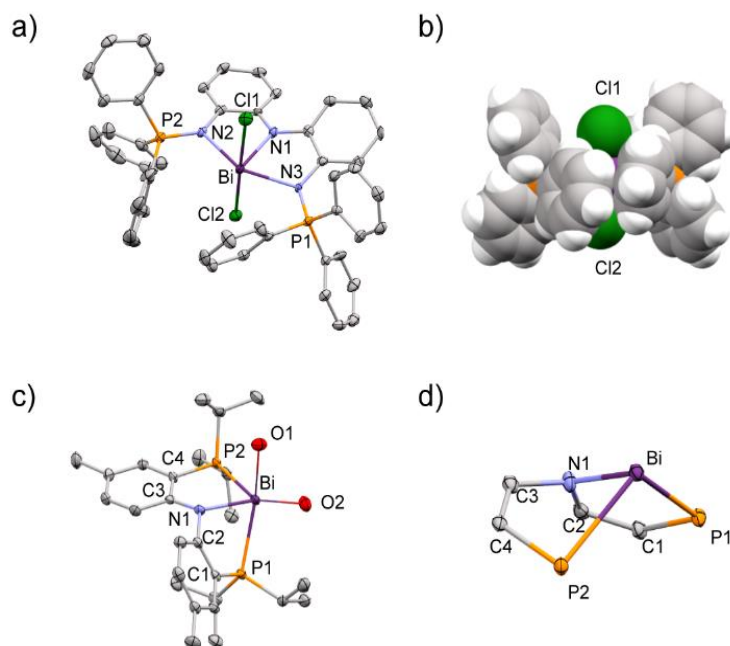


**Figure 2** a) Solid state structure of **1**(CH<sub>2</sub>Cl<sub>2</sub>)<sub>2</sub>. Ellipsoids are drawn at the 50% probability level. Hydrogen atoms and solvent molecules have been omitted. b) Space-filling model (vdW radii used) of **1**. c) Solid state structure of **2b**. Ellipsoids are drawn at the 50% probability level. Hydrogen atoms and non-essential portions of the triflate anions have been omitted. d) Truncated view of the coordination environment around Bi in **2b**.

We therefore prepared a related derivative, **2c**, by performing an anion exchange using AgOSO<sub>2</sub>CF<sub>3</sub> (AgOTf) as a triflate source.<sup>53, 54</sup> Compound **2b**, isolated in 58% yield, proved to be thermally unstable, with DCM solutions decomposing to a mixture of products that include **2a** (by solvent activation) within hours (Figure S9, ESI). The <sup>1</sup>H NMR spectrum of this compound shows a single environment and relatively sharp resonances for the isopropyl groups, consistent with a high-symmetry time-averaged planar ligand configuration. Notably, the <sup>31</sup>P NMR resonance for **2b** is also sharper and shifted dramatically downfield to 95.1 ppm compared to **2a** (41.5 ppm). The <sup>19</sup>F NMR spectrum of **2b** shows a resonance at -78.05 ppm, which is close to the value for [NBu<sub>4</sub>][OTf] (-78.50 ppm).<sup>55</sup> Collectively, these spectral features imply weak

interactions between the bismuth centre and the triflate groups in solution. The resulting increase in the electrophilicity at the metal presumably engenders more robust P-Bi interactions, explaining the sharper resonances observed for **2b** compared to **2a**.

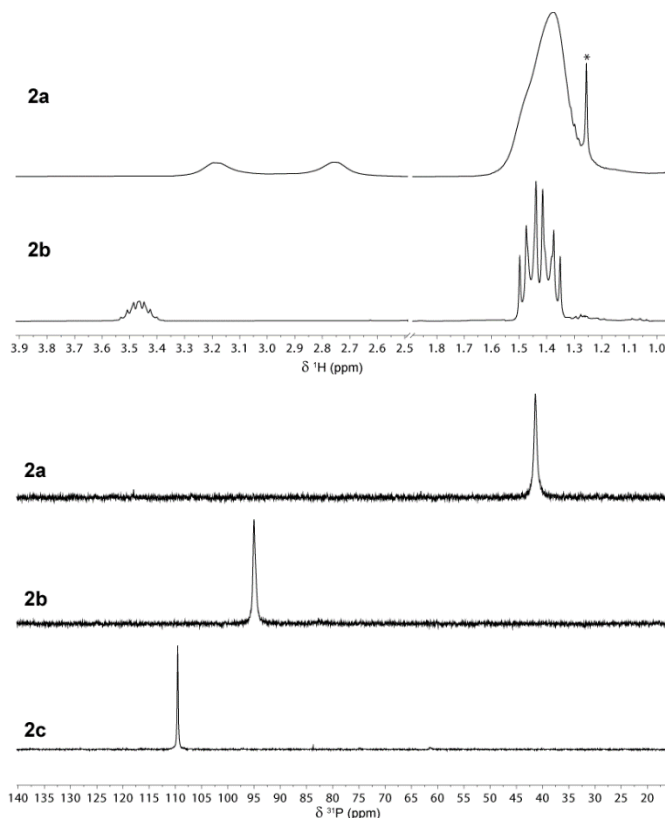


**Figure 3** Top: Portion of the  $^1\text{H}$  NMR spectra of **2a** and **2b** in  $\text{CDCl}_3$ . Asterisk denotes trace contamination from pentane (low solubility of **2a** accentuates NMR solvent impurities). Bottom:  $^{31}\text{P}$  NMR spectra of **2a**, **2b** and **2c**.

Cooling a concentrated DCM solution of **2b** to  $-30\text{ }^\circ\text{C}$  allowed isolation of single-crystals amenable to X-ray diffraction. In contrast to the structure of previously reported **PNP-M** complexes ( $\text{M} = \text{Al}, \text{Ga}, \text{In}, \text{Sn}$ ),<sup>45, 47</sup> and the preceding discussion about solution-phase structure, **2b** shows a distinctly bent ligand in the solid state with a P1-Bi-P2 angle of  $105.76(3)^\circ$  (Figure 2c, d). These phase-dependent structural outcomes point to facile interconversion between the two geometries, such that solvent and lattice effects can easily favour one or the other outcome, which is in line with the reportedly small inversion barriers at hypervalent bismuth centres.<sup>56, 57</sup> Notably, the P1-Bi bond length in **2b** [ $2.6549(8)\text{ \AA}$ ] is nearly  $0.1\text{ \AA}$  shorter than the P2-Bi bond length [ $2.7306(8)\text{ \AA}$ ], supporting the aforementioned possibility of asymmetry in the strength of P-Bi interactions (Scheme 1c). Two long Bi-O interactions are also located *cis* to one another [ $\text{O-Bi-O} = 119.99(8)^\circ$ ] and opposite the Bi-N1 and Bi-P1 bonds, with the deviation from  $90^\circ$  being

a result of a stereochemically active lone pair. The average Bi-O distances in **2b** (ca. 2.72 Å) are within the sum of the van der Waals radii (3.59 Å) but significantly longer than the sum of the covalent radii for the two elements (2.14 Å), suggesting at least partial ionic character. Indeed, the crystallographically determined structural features of **2b** are well-reproduced (Table 1) by DFT calculations performed on the hypothetical triflate-free dication [**PNP-Bi**]<sup>2+</sup>.

**Table 1** Selected bond lengths (Å) and angles (°) in the solid state structures of **1** and **2b**, and the calculated (B3LYP-D3BJ/aug-cc-pVDZ-PP) structure of triflate-free [**PNP-Bi**]<sup>2+</sup>.

Parameter	<b>1</b> •(CH <sub>2</sub> Cl <sub>2</sub> ) <sub>2</sub>	<b>2b</b>	[ <b>PNP-Bi</b> ] <sup>2+</sup>
Bi-N	2.165(5) N1 2.358(5) N2 2.371(5) N3	2.215(3)	2.194
Bi-P	-	2.6549(8) P1 2.7306(8) P2	2.652 2.715
Bi-Cl	2.703(1) Cl1 2.721(1) Cl2	-	-
Bi-O	-	2.739(2) O1 2.693(3) O2	-
N-Bi-N	74.0(2) N1, N2 73.1(2) N1, N3 146.6(2) N2, N3	-	-
P-Bi-P	-	105.76(3) P1, P2	108.0
N-Bi-P	-	73.12(7) N1, P1 76.82(7) N1, P2	79.3 76.9
Cl-Bi-Cl	175.75(5) Cl1, Cl2	-	-
O-Bi-O	-	119.99(8) O1, O2	-

In light of the above, we hypothesized that the Bi centre in **2b** is considerably more electrophilic than in **2a**, making the triflate derivative thermally more reactive and therefore quite unstable towards decomposition via solvent activation or adventitious impurities. To explore this possibility, we converted **2a** to **2c** using [Et<sub>3</sub>Si(PhMe)][B(C<sub>6</sub>F<sub>5</sub>)<sub>4</sub>] as a metathesis reagent (Scheme 1b). The <sup>31</sup>P NMR resonance of the resulting compound is not only the sharpest, but also the most downfield of all derivatives at 109.5 ppm (Figure 3, bottom) due to the very weakly-coordinating nature of the perfluoroarylborate anion, which minimally quenches the electrophilicity at bismuth. Compound **2c** also proved to be very thermally unstable even in solutions of 1,2-difluorobenzene or as a solid, precluding isolation and complete characterization. Its dissolution in DCM or CDCl<sub>3</sub> resulted in reformation of **2a** over time, evidencing solvent activation. High reactivity for analogous bismuth electrophiles has been reported previously, including CH and CO activation and polymerization via activation of π systems and ethers.<sup>58-62</sup> In line with these reports, solution of **2c** in THF rapidly turn into insoluble purple gels via catalytic ring-opening polymerization of the cyclic ether (Figure S15, ESI).

In summary, we have reported the first example of a p-block complex featuring the rigid  $P_2N_3$  framework in **1**, which enforces a planar ligand environment at the bismuth centre in both the solution and solid phases. We also report the first **PNP-Bi** complexes (**2a-c**), which show remarkable structural dynamism as a function of phase and substitution at the metal. For example, in solution, **2a** appears to have a low-symmetry, bent ligand arrangement and **2b** a high-symmetry planar arrangement, and potentially dissociated anions. However, in the solid phase **2b** clearly shows an asymmetric bent ligand environment. Preliminary studies show that **2b** and **2c** are potent electrophiles, which renders them thermally unstable. We are now exploring the reactivity of these compounds as convenient precursors to sterically shielded Bi(I) centres (e.g. derived from **1** and **2a**) and Lewis acid catalysts (e.g. derived from **2b** and **2c**).

### Conflicts of interest

There are no conflicts to declare.

### Acknowledgments

We acknowledge the Natural Sciences and Engineering Resesarch Council (NSERC) of Canada, the Canada Foundation for Innovation (CFI), the Nova Scotia Research and Innovation Trust (NSRIT), and Dalhousie University for research funding. K.M.M. acknowledges the Vanier Canada Graduate Scholarships Program and the Walter C. Sumner Memorial Fellowships Program for funding. M.B.K. acknowledges the Sipekne'katic First Nation for a research stipend.

### References

1. A. J. Arduengo, C. A. Stewart, F. Davidson, D. A. Dixon, J. Y. Becker, S. A. Culley and M. B. Mizen, *J. Am. Chem. Soc.*, 1987, **109**, 627-647.
2. A. J. Arduengo and C. A. Stewart, *Chem. Rev.*, 1994, **94**, 1215-1237.
3. N. L. Dunn, M. Ha and A. T. Radosevich, *J. Am. Chem. Soc.*, 2012, **134**, 11330-11333.
4. Y.-C. Lin, E. Hatzakis, S. M. McCarthy, K. D. Reichl, T.-Y. Lai, H. P. Yennawar and A. T. Radosevich, *J. Am. Chem. Soc.*, 2017, **139**, 6008-6016.
5. T. P. Robinson, D. M. De Rosa, S. Aldridge and J. M. Goicoechea, *Angew. Chem. Int. Ed.*, 2015, **54**, 13758-13763.
6. S. Volodarsky and R. Dobrovetsky, *Chem. Commun.*, 2018, **54**, 6931-6934.
7. F. Ebner and L. Greb, *J. Am. Chem. Soc.*, 2018, **140**, 17409-17412.



8. S. S. Chitnis, J. H. W. LaFortune, H. Cummings, L. L. Liu, R. Andrews and D. W. Stephan, *Organometallics*, 2018, **37**, 4540-4544.
9. S. S. Chitnis, F. Krischer and D. W. Stephan, *Chem. Eur. J.*, 2018, **24**, 6543-6546.
10. R. J. Andrews, S. S. Chitnis and D. W. Stephan, *Chem. Commun.*, 2019, **55**, 5599-5602.
11. M. B. Kindervater, K. M. Marczenko, U. Werner-Zwanziger and S. S. Chitnis, *Angew. Chem. Int. Ed.*, 2019, **58**, 7850-7855.
12. K. M. Marczenko, J. A. Zurakowski, K. L. Bamford, J. W. M. MacMillan and S. S. Chitnis, *Angew. Chem. Int. Ed.*, 2019, **58**, 18096-18101.
13. K. M. Marczenko, J. A. Zurakowski, M. B. Kindervater, S. Jee, T. Hynes, N. Roberts, S. Park, U. Werner-Zwanziger, M. Lumsden, D. N. Langelaan and S. S. Chitnis, *Chem. Eur. J.*, 2019, **25**, 16414-16424.
14. K. M. Marczenko and S. S. Chitnis, *Chem. Commun.*, 2020, DOI: 10.1039/D0CC00254B.
15. G. Strimb, A. Pollnitz, C. I. Rat and C. Silvestru, *Dalton Trans.*, 2015, **44**, 9927-9942.
16. A. P. Soran, C. Silvestru, H. J. Breunig, G. Balazs and J. C. Green, *Organometallics*, 2007, **26**, 1196-1203.
17. P. Simon, R. Jambor, A. Ruzicka and L. Dostal, *J. Organomet. Chem.*, 2013, **740**, 98-103.
18. P. Simon, F. de Proft, R. Jambor, A. Ruzicka and L. Dostal, *Angew. Chem., Int. Ed.*, 2010, **49**, 5468-5471, S5468/5461-S5468/5466.
19. D. R. Kindra, I. J. Casely, J. W. Ziller and W. J. Evans, *Chem. - Eur. J.*, 2014, **20**, 15242-15247.
20. D. R. Kindra, I. J. Casely, M. E. Fieser, J. W. Ziller, F. Furche and W. J. Evans, *J. Am. Chem. Soc.*, 2013, **135**, 7777-7787.
21. L. Dostal, R. Jambor, A. Ruzicka, R. Jirasko, E. Cernoskova, L. Benes and F. de Proft, *Organometallics*, 2010, **29**, 4486-4490.
22. I. J. Casely, J. W. Ziller, M. Fang, F. Furche and W. J. Evans, *J. Am. Chem. Soc.*, 2011, **133**, 5244-5247.
23. H. J. Breunig, M. G. Nema, C. Silvestru, A. P. Soran and R. A. Varga, *Dalton Trans.*, 2010, **39**, 11277-11284.
24. L. Balazs, H. J. Breunig, E. Lork, A. Soran and C. Silvestru, *Inorg. Chem.*, 2006, **45**, 2341-2346.
25. D. A. Atwood, A. H. Cowley and J. Ruiz, *Inorg. Chim. Acta*, 1992, **198-200**, 271-274.
26. C. I. Raț, C. Silvestru and H. J. Breunig, *Coord. Chem. Rev.*, 2013, **257**, 818-879.
27. L. Dostál, R. Jambor, A. Růžicka, M. Erben, R. Jirásko, E. Černošková and J. Holeček, *Organometallics*, 2009, **28**, 2633-2636.
28. W.-C. Xiao, Y.-W. Tao and G.-G. Luo, *Int. J. Hydrogen Energy*, 2020, **45**, 8177-8185.
29. F. Wang, O. Planas and J. Cornella, *J. Am. Chem. Soc.*, 2019, **141**, 4235-4240.

30. C. A. Stewart, J. C. Calabrese and A. J. Arduengo, *J. Am. Chem. Soc.*, 1985, **107**, 3397-3398.
31. L. Dostal, P. Novak, R. Jambor, A. Ruazicka, I. Cisarova, R. Jirasko and J. Holecek, *Organometallics*, 2007, **26**, 2911-2917.
32. I. Vranova, R. Jambor, A. Ruzicka, A. Hoffmann, S. Herres-Pawlis and L. Dostal, *Dalton Trans.*, 2015, **44**, 395-400.
33. P. Molina, M. J. Lidon and A. Tarraga, *Tetrahedron*, 1994, **50**, 10029-10036.
34. A. Maurer, D. Fenske, J. Beck, W. Hiller, J. Straehle, E. Boehm and K. Dehnicke, *Z. Naturforsch., B: Chem. Sci.*, 1988, **43**, 5-11.
35. T. Cheisson, L. Ricard, F. W. Heinemann, K. Meyer, A. Auffrant and G. Nocton, *Inorg. Chem.*, 2018, **57**, 9230-9240.
36. R. Cariou, T. W. Graham and D. W. Stephan, *Dalton Trans.*, 2013, **42**, 4237-4239.
37. R. Cariou, T. W. Graham, F. Dahcheh and D. W. Stephan, *Dalton Trans.*, 2011, **40**, 5419-5422.
38. R. Cariou, F. Dahcheh, T. W. Graham and D. W. Stephan, *Dalton Trans.*, 2011, **40**, 4918-4925.
39. C. Bakewell, A. J. P. White, N. J. Long and C. K. Williams, *Inorg. Chem.*, 2015, **54**, 2204-2212.
40. C. Bakewell, A. J. P. White, N. J. Long and C. K. Williams, *Angew. Chem., Int. Ed.*, 2014, **53**, 9226-9230.
41. C. Bakewell, T.-P.-A. Cao, N. Long, X. F. Le Goff, A. Auffrant and C. K. Williams, *J. Am. Chem. Soc.*, 2012, **134**, 20577-20580.
42. L. Fan, B. M. Foxman and O. V. Ozerov, *Organometallics*, 2004, **23**, 326-328.
43. K. R. D. Johnson and P. G. Hayes, *Inorg. Chim. Acta*, 2014, **422**, 209-217.
44. J. Henning, H. Schubert, K. Eichele, F. Winter, R. Poettgen, H. A. Mayer and L. Wesemann, *Inorg. Chem.*, 2012, **51**, 5787-5794.
45. K. Yurkerwich and G. Parkin, *Inorg. Chim. Acta*, 2010, **364**, 157-161.
46. P.-Y. Lee and L.-C. Liang, *Inorg. Chem.*, 2009, **48**, 5480-5487.
47. J. C. DeMott, C. Guo, B. M. Foxman, D. V. Yandulov and O. V. Ozerov, *Mendeleev Commun.*, 2007, **17**, 63-65.
48. B. C. Bailey, A. R. Fout, H. Fan, J. Tomaszewski, J. C. Huffman and D. J. Mindiola, *Angew. Chem., Int. Ed.*, 2007, **46**, 8246-8249.
49. J. C. DeMott, P. Surawatanawong, S. M. Barnett, C.-H. Chen, B. M. Foxman and O. V. Ozerov, *Dalton Trans.*, 2011, **40**, 11562-11570.
50. D. E. Herbert, A. D. Miller and O. V. Ozerov, *Chemistry*, 2012, **18**, 7696-7704.
51. P. S. Nejman, T. E. Curzon, M. Bühl, D. McKay, J. D. Woollins, S. E. Ashbrook, D. B. Cordes, A. M. Z. Slawin and P. Kilian, *Inorg. Chem.*, 2020, DOI: 10.1021/acs.inorgchem.0c00317.
52. S. S. Chitnis, N. Burford, A. Decken and M. J. Ferguson, *Inorg. Chem.*, 2013, **52**, 7242-7248.

53. S. S. Chitnis, N. Burford and M. J. Ferguson, *Angew. Chem. Int. Ed.*, 2013, **52**, 2042-2045.
54. S. S. Chitnis, A. P. M. Robertson, N. Burford, B. O. Patrick, R. McDonald and M. J. Ferguson, *Chem. Sci.*, 2015, **6**, 6545-6555.
55. A. M. Ullman and D. G. Nocera, *J. Am. Chem. Soc.*, 2013, **135**, 15053-15061.
56. K.-y. Akiba and Y. Yamamoto, *Heteroat. Chem*, 2007, **18**, 161-175.
57. Y. Yamamoto, X. Chen, S. Kojima, K. Ohdoi, M. Kitano, Y. Doi and K.-y. Akiba, *J. Am. Chem. Soc.*, 1995, **117**, 3922-3932.
58. C. Lichtenberg, F. Pan, T. P. Spaniol, U. Englert and J. Okuda, *Angew. Chem. Int. Ed.*, 2012, **51**, 13011-13015.
59. B. Ritschel, J. Poater, H. Dengel, F. M. Bickelhaupt and C. Lichtenberg, *Angew. Chem. Int. Ed.*, 2018, **57**, 3825-3829.
60. J. Ramler, J. Poater, F. Hirsch, B. Ritschel, I. Fischer, F. M. Bickelhaupt and C. Lichtenberg, *Chem. Sci.*, 2019, **10**, 4169-4176.
61. S. Balasubramaniam, S. Kumar, A. P. Andrews, B. Varghese, E. D. Jemmis and A. Venugopal, *Eur. J. Inorg. Chem.*, 2019, **2019**, 3265-3269.
62. R. J. Schwamm, B. M. Day, M. P. Coles and C. M. Fitchett, *Inorg. Chem.*, 2014, **53**, 3778-3787.